

# Highly sensitive and easy-to-use SQUID sensors

D. Drung, C. Aßmann, J. Beyer, A. Kirste, M. Peters, F. Ruede, and Th. Schurig

**Abstract**—We have developed a novel family of low-noise superconducting quantum interference devices (SQUIDs) to cover a wide range of applications. These sensors are robust and easy to use without compromising noise performance. They are optimized for operation with our high-speed direct-coupled flux-locked loop (FLL) electronics XXF-1. For the readout of cryogenic detectors, series arrays of 16 SQUIDs with  $\leq 3$  nH input inductance were designed which can be cooled down and operated in the Earth's field without magnetic shield. A compact gradiometric design allows the chips to be mounted directly on a Cu block at the cold stage of a mK cryostat without degradation in noise. A current noise level of  $9 \text{ pA}/\sqrt{\text{Hz}}$  or  $5 \text{ pA}/\sqrt{\text{Hz}}$  is achieved at 4.2 K or 300 mK, respectively. Ultra-high-speed operation was demonstrated by using a cold FLL electronics prototype in close proximity to the SQUID array. An extremely high FLL bandwidth of 350 MHz was achieved which outperforms any flux-locked SQUID before by more than an order of magnitude. For applications requiring a larger input inductance of up to 2  $\mu\text{H}$ , integrated two-stage sensors were developed consisting of a single front-end SQUID with double-transformer coupling read out by a 16-SQUID array. These sensors are very convenient to use as their voltage-flux characteristic is essentially single-SQUID-like. Devices optimized for 4.2 K operation have a coupled energy resolution around 50 times Planck's constant  $h$ . Heavily shunted devices for low-temperature operation typically achieve  $80 h$  or  $8 h$  at 4.2 K or 300 mK, respectively. An optional current limiter (Q-spoiler) at the input reduces the input current in pulsed applications like nuclear magnetic resonance or magnetorelaxometry. Integrated rf filters and resistor-capacitor shunts across the input coil result in smooth, well-behaved voltage-flux characteristics even at low temperatures  $\ll 4.2$  K. For magnetic field sensing applications, integrated miniature multiloop magnetometers were designed with maximized field resolution. For a 3 mm  $\times$  3 mm chip size, a noise level of  $3.6 \text{ fT}/\sqrt{\text{Hz}}$  is obtained at 4.2 K.

**Index Terms**—Current sensor, magnetometer, series SQUID array, two-stage SQUID

## I. INTRODUCTION

**B**ASICALLY, a dc superconducting quantum interference device (SQUID) is a magnetic field sensor converting the flux  $\Phi$  threading the SQUID loop into a voltage  $V$  across the device. However, in many applications the SQUID is used as a low noise current amplifier rather than a magnetic field sensor, e.g., to sense the current in a superconducting pickup coil or to read out cryogenic detectors.

Manuscript received August 22, 2006. This work was supported in part by the German Federal Ministry of Economics and Technology (BMW).i.

The authors are with the Physikalisch-Technische Bundesanstalt (PTB), Abbestrasse 2-12, D-10587 Berlin, Germany (phone: +49-30-3481-7342; fax: +49-30-3481-7490; e-mail: dietmar.drung@ptb.de).

A figure of merit for SQUID current sensors is the coupled energy resolution  $\epsilon_c = S_I L_{in}/2$  where  $S_I$  is the input-referred current noise and  $L_{in}$  is the input inductance. Modern low-transition-temperature (low- $T_c$ ) dc SQUIDs typically have an inductance  $L$  of 100 pH and a junction capacitance  $C$  of 1 pF. According to theory [1] the energy resolution is approximately equal to  $16 k_B T (LC)^{1/2}/k^2$  where  $k_B$  is the Boltzmann constant,  $T$  is the operation temperature, and  $k$  is the coupling constant between input coil and SQUID loop. Thus, a well-coupled dc SQUID operated in liquid helium could have an energy resolution below 20 times Planck's constant  $h$ .

Commonly, a spiral input coil with up to about 100 turns is wound on the SQUID "washer" in order to obtain the desired input inductance (typically 1  $\mu\text{H}$  for wire-wound pickup coils) [2]. This planar coupling scheme allows a very efficient coupling with  $k$  close to unity, but leads to parasitic microwave resonances which increase the SQUID noise by mixing-down effects. This becomes even more critical if the SQUID inductance is lowered in order to improve the energy resolution. Although schemes have been developed to damp these resonances [2], coupled dc SQUIDs have generally a (much) higher noise level than predicted by the simple theory. A coupled energy resolution below  $100 h$  at 4.2 K is difficult to achieve with high- $L_{in}$  SQUIDs.

In the past, we have used our integrated multiloop magnetometers as current sensors by adding a wire-wound or integrated input coil. Noise levels below  $1 \text{ pA}/\sqrt{\text{Hz}}$  and a coupled energy resolution down to about  $200 h$  were achieved at 4.2 K [3] which are adequate for most applications. However, our multiloop SQUIDs require strong magnetic shielding because of their high sensitivity to magnetic fields. Furthermore, the noise does not improve noticeably when operating the devices at mK temperatures because they were designed for a high value of the hysteresis parameter  $\beta_c = 2\pi I_0 R^2 C/\Phi_0 > 1$  in order to get a large SQUID signal ( $I_0$  is the critical current of the Josephson junctions,  $R$  is the shunt resistance in parallel to each junction, and  $\Phi_0$  is the flux quantum). Finally, the slew rate is sub-optimal because additional positive feedback (APF) was used to enhance  $V_\Phi \equiv \partial V/\partial \Phi$  for enabling direct readout [4].

Therefore, we have developed a novel family of current sensors which are insensitive to external magnetic fields, allow high slew rates, and have a better energy resolution in particular at mK temperatures. The basic design criteria are discussed in Sec. II, followed by a description of the main devices of the sensor family (Sec. III to Sec. V).

## II. BASIC DESIGN CONSIDERATIONS

Series SQUID arrays [5] are ideal in terms of slew rate because the linear flux range of the  $V\text{-}\Phi$  characteristic is not decreased as with APF. Provided that all individual SQUIDs of the array are biased at the same working point and that the same flux is coupled into each of it, the array behaves like a single SQUID with enlarged voltage signal. A SQUID array can easily be read out directly with a room temperature amplifier. However, when it is cooled down in a high magnetic field such as the Earth's field, the  $V\text{-}\Phi$  characteristic may be strongly distorted due to trapped flux which leads to variations in the flux biases of the SQUIDs. Therefore, the linewidth in the array should be chosen such that vortices cannot enter the Nb films during cool-down, and one should avoid closed superconducting loops which can trap flux due to screening or noise currents. The latter condition means that arrays of parallel gradiometer SQUIDs [6] should not be used if large cooling fields are desired.

It was recently shown [7] that complete vortex expulsion from narrow superconducting strips of width  $w$  occurs if the cooling field  $B_{\text{cool}}$  is kept in the range  $B_{\text{cool}} \lesssim \Phi_0/w^2$ . Thus, a maximum linewidth of about  $5 \mu\text{m}$  should be used to reliably cool down a SQUID array in the Earth's field (a prerequisite for unshielded operation or for configurations where a Nb shield is used without an extra high-permeability shield). For our  $2.5 \mu\text{m}$  technology this means that only a single-turn input coil can be realized which represents a severe design constraint. To realize a series array with a  $1 \mu\text{H}$  input inductance one would need about 10000 SQUIDs with  $L \approx 100 \text{ pH}$ !

Therefore, we have implemented the double-transformer scheme [8], [9] in our second sensor generation C2 [10]. In this scheme, the input coil of the SQUID (or the SQUID array) is coupled to a large input transformer, and a low SQUID inductance can easily be matched to a high input inductance. As shown in Fig. 1, a double-transformer SQUID is equivalent to a conventional SQUID of inductance  $L$ , input inductance  $L_{\text{in}}$ , and mutual inductance  $M$ . For ideal coupling of the individual transformers  $k_{12} = M_{12}/(L_1L_2)^{1/2} = 1$  and  $k_{34} = M_{34}/(L_3L_4)^{1/2} = 1$ , perfect overall coupling  $k = M/(L_{\text{in}}L)^{1/2} = 1$  is obtained. However, the overall coupling degrades rapidly with decreasing  $k_{12}$  and  $k_{34}$ . Assuming for simplicity  $L_2 = L_3$  and  $k_{12} = k_{34} = k_0$ , the overall coupling constant is given by  $k = k_0^2/(2-k_0^2)$ . Thus, for reasonable individual coupling constants  $k_0$  of 90% or 80% the overall coupling constant  $k$  is low 68% or 47%, respectively.

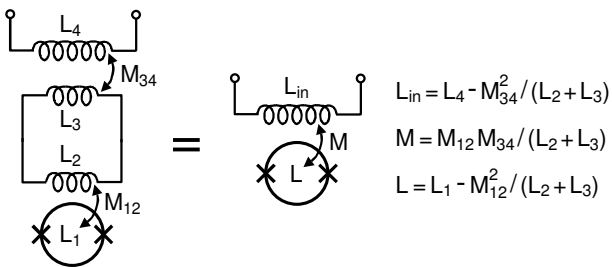


Fig. 1. Basic equivalent circuit of a double-transformer SQUID.

For our C2 sensors with double transformer the input transformer had to be placed far away from the SQUID array in order to minimize the effect of stray fields from the large superconducting areas of the transformer [10]. The stray inductance of the interconnect lines mainly limited the sensor performance. It resulted in a low overall coupling constant  $k \lesssim 40\%$  and a degraded energy resolution  $\epsilon_c$  of typically  $450 h$  at 4.2 K. The corresponding current noise level was  $0.63 \text{ pA}/\sqrt{\text{Hz}}$  for  $L_{\text{in}} = 1.5 \mu\text{H}$ . On the other hand, the current noise level of the array alone (i.e., without input transformer) was  $10 \text{ pA}/\sqrt{\text{Hz}}$  or  $6 \text{ pA}/\sqrt{\text{Hz}}$  at 4.2 K or 300 mK, respectively, which is adequate for the readout of transition-edge sensors [11]. Therefore, we decided to split our sensor development into two directions: (1) high- $L_{\text{in}}$  sensors optimized with respect to noise performance for applications in the traditional inductance regime of  $\approx 1 \mu\text{H}$ , and (2) "pure" SQUID arrays with low  $L_{\text{in}} < 10 \text{ nH}$  for applications requiring a high dynamic performance such as the readout of transition-edge sensors. We first developed a prototype series C3 consisting of a few different sensors in order to test the basic function of our SQUID concepts. After the successful test of C3, we designed the final mask set C4 with a large variety of devices.

## III. SENSORS WITH HIGH INPUT INDUCTANCE

If a single SQUID is used for the double transformer scheme instead of a SQUID array, the input transformer can be placed close to the SQUID and a good overall coupling can be achieved [9]. On the other hand, direct readout becomes more difficult than with the SQUID array. At 4.2 K, APF combined with bias current feedback (BCF) is a useful way to solve the readout problem [12]. However, if the device is cooled to mK temperatures in order to improve the energy resolution, APF and BCF might suppress the preamplifier noise insufficiently and the overall noise might degrade. In this case, a two-stage readout with a second SQUID used as a low-noise preamplifier is the preferred choice [4], [13].

The main parameter of a two-stage SQUID is the small-signal flux gain  $G_\Phi \equiv \partial\Phi_{\text{amp}}/\partial\Phi$  at the working point W. It specifies how much flux  $\partial\Phi_{\text{amp}}$  is coupled into the amplifier SQUID if the flux in the front-end SQUID is changed by a small amount  $\partial\Phi$ . The contribution of the amplifier SQUID to the overall flux noise decreases with the flux gain. Consequently, a high flux gain and a low flux noise of the amplifier SQUID (including contributions from the room temperature amplifier) are desirable. As the flux noise density  $S_\Phi$  of series SQUID arrays decreases with the number of SQUIDs, they are nearly ideal preamplifiers [14], [15].

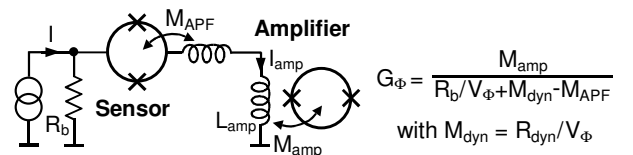


Fig. 2. Basic circuit of a two-stage SQUID with APF. For the second stage, a series SQUID array may be preferably used rather than a single SQUID.

In order to obtain single-SQUID-like characteristics even at high  $G_\Phi$ , we implemented APF in our two-stage SQUIDs (see Fig. 2). APF requires just a superconducting coil between first and second stage; thus, it produces no extra noise. The front-end SQUID is voltage biased, i.e., the bias resistance  $R_b = R/10$  is made much smaller than the dynamic resistance  $R_{\text{dyn}}$  of the SQUID [4]. The flux bias  $\Phi_x$  of the amplifier SQUID is chosen such that it is operated in a low-noise, linear region of its  $V$ - $\Phi$  characteristic. The output current swing  $\Delta I$  of the front-end SQUID produces a proportional flux swing  $\Delta\Phi_{\text{amp}} = M_{\text{amp}}\Delta I$  in the amplifier SQUID where  $M_{\text{amp}}$  is the input mutual inductance of the second-stage.  $\Delta\Phi_{\text{amp}}$  should be kept below about  $\Phi_0/2$  to get a user-friendly overall transfer characteristics [15]. This is illustrated in Fig. 3 by the overall transfer characteristics of a two-stage device of our third sensor generation C3 for different values of the amplifier flux bias. The relatively small current swing  $\Delta I \approx 4.5 \mu\text{A}$  modulates the amplifier characteristics by only 20% of a flux quantum. Thus, the overall characteristic is single-SQUID-like for the properly chosen flux bias  $\Phi_x$  in Figs. 3 (a) and (c). In

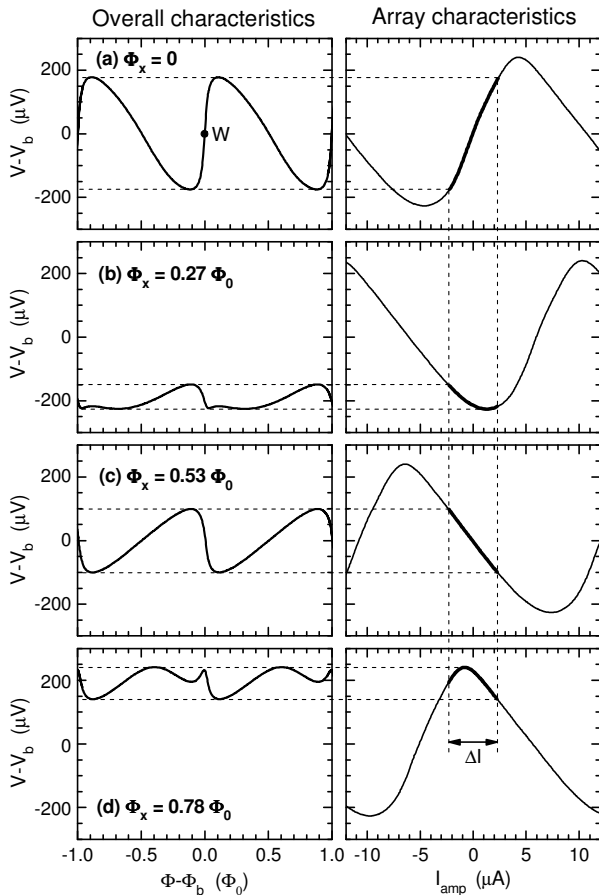


Fig. 3. Overall  $V$ - $\Phi$  characteristics (left) and array characteristics (right) of a two-stage sensor C3XL116 with APF for four representative values of the array flux bias  $\Phi_x$ . The device parameters were optimized for 4.2 K operation ( $\beta_c \approx 0.8$ ). The optimum working point W is indicated by a circle. Dashed lines show the output current swing  $\Delta I \approx 4.5 \mu\text{A}$  of the front-end SQUID. The array is loaded by the  $50 \Omega$  input resistance of the room temperature amplifier leading to a nearly triangular array characteristic [16]. The asymmetry in the array characteristic results from the asymmetric bias current feed which lowers the dynamic resistance at the positive slope [17].

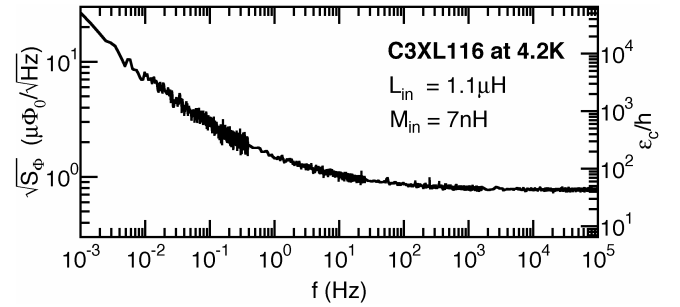


Fig. 4. Flux noise spectrum of the C3XL116 sensor of Fig. 3 at the optimum working point W. The device was operated with the XXF-1 readout electronics [16]. The right-hand scale shows the coupled energy resolution.

contrast, for  $\Phi_x$  near the extreme values of the amplifier  $V$ - $\Phi$  characteristic, the overall characteristic is unusable – see Figs. 3 (b) and (d).

For a user-friendly sensor, the flux bias  $\Phi_x$  should remain constant independent of magnetic background and thermal cycling. This condition is fulfilled for our devices which are very insensitive to magnetic fields due to a highly gradiometric design. The parasitic area of the array SQUIDs is of the order of  $1 \mu\text{m}^2$  in all field directions corresponding to a parasitic field sensitivity of  $2 \text{ mT}/\Phi_0$ . Furthermore, the arrays do not trap flux even when cooling them in the Earth field due to a  $5 \mu\text{m}$  linewidth of the SQUID loops.

The noise spectrum of the C3XL116 sensor of Fig. 3 is depicted in Fig. 4. The white flux noise level at 4.2 K was as low as  $0.78 \mu\Phi_0/\sqrt{\text{Hz}}$  corresponding to a very low current noise level of  $0.23 \text{ pA}/\sqrt{\text{Hz}}$  and a coupled energy resolution of  $44 h$ . We estimated the effective SQUID inductance to be  $L \approx 80 \text{ pH}$  and the overall coupling constant  $k \approx 74\%$ . The effect of second-stage noise was negligible due to a low array flux noise of  $\approx 0.4 \mu\Phi_0/\sqrt{\text{Hz}}$  and a high flux gain  $G_\Phi \approx 3$ . When cooling the device to 300 mK, the white noise dropped to  $6.5 h$ ; however, due to the relatively high  $\beta_c$  close to unity, the array characteristic became strongly resonance-distorted although the transfer characteristic of the front-end SQUID was still smooth and well-behaved. For low-temperature operation, we had to select a lower shunt resistance for the array SQUIDs ( $\beta_c \approx 0.25$ ). As for our C3 devices this also decreases the  $\beta_c$  of the front-end SQUID, the noise level increases to typically  $80 h$  or  $8 h$  at 4.2 K or 300 mK, respectively. Therefore, in our latest sensor generation C4 we added the option to make the  $\beta_c$  of the front-end SQUID twice as high as that of the array SQUIDs. Furthermore, we implemented extra shunt resistors in the array in order to allow a higher  $\beta_c$  and a correspondingly lower noise level. Measurements are under preparation to test the success of these design changes.

At 4.2 K, the  $1/f$  corner frequency of the flux noise is typically around 2 Hz. However, the low-frequency noise increases when lowering the temperature. Typically, there is a crossover of the 4.2 K and 300 mK noise spectra between 10 Hz and 100 Hz [16]. The reason for this is yet unclear, but increased low-frequency noise at very low temperatures was also reported in literature [13]. Bias current reversal [4] did

not noticeably improve the low-frequency noise thus excluding critical-current fluctuations as the source. Furthermore, we did not observe a systematic dependence on the material of the insulation layer ( $\text{SiO}_2$  vs.  $\text{Si}_3\text{N}_4$ ). In our C4 mask set, we added a series of test SQUIDs with different inductances, junction sizes, and shunt resistances in order to investigate the problem.

Fig. 5 shows the design and simplified circuit diagram of our integrated two-stage sensor. All SQUIDs on the chip are realized as gradiometers in order to minimize the sensitivity to magnetic fields. A high tolerable cooling field of the order of  $60 \mu\text{T}$  ensures unshielded cool-down and operation in the Earth field. An additional feedback transformer in series to the input coil allows one to null the input current rather than the flux in the SQUID if desired [2]. To avoid large currents in the input coil, an optional on-chip current limiter (Q-spoiler) may be used. It is realized by a series array of 16 unshunted 20 pH SQUIDs connected in series with the input coil.

The input transformer is realized by two large washers connected as a first-order series gradiometer. Each washer is shunted by an individual  $R$ - $C$  shunt [15] which provides

efficient damping even at low values of the source impedance. With a single  $R$ - $C$  shunt across the input coil the damping effect would decrease with the source impedance, and disappear with shorted input coil. A higher gradiometer order is not needed for the input transformer as the area formed by the commonly used input screw terminals dominates the parasitic field-sensitive area when a superconducting load is connected to the sensor input.

The front-end SQUID is realized as a second-order parallel gradiometer. Feedback, APF and input flux are coupled into separate washers in order to minimize the coupling between feedback/APF and input. For our C3XL116 sensor, the variation in the feedback coil mutual inductance is only 3.7% for the extreme cases of open and shorted input coil. For the C4 sensors we expect an even smaller variation.

All lines connecting the sensor chip with the room temperature readout electronics are passed through on-chip rf filters. The two-stage device requires a minimum of seven wires between room temperature and cryogenic part, i.e., only two extra wires compared to a single-stage device (+I and +FX in Fig. 5; -IFX may be connected with -V on the chip carrier). Only the three wires between the sensor output and the room temperature preamplifier have to have a low resistance below a few Ohms ( $\pm V$  in Fig. 5 plus an extra ground wire [18]).

An attractive feature is that no separate heater resistor (and consequently no extra wire) is needed to expel trapped magnetic flux. In our setup the heater current is directly sent through the SQUID array. If the chip is immersed in liquid helium, an average power density of about  $1 \text{ W/cm}^2$  (i.e., about  $0.1 \text{ W}$  for our  $3 \text{ mm} \times 3 \text{ mm}$  chips) is sufficient to heat up the complete chip above the critical temperature of the Nb films. Obviously, in vacuum the required heating power is lower. During the heating process, the voltage drop across the SQUID array is typically 5 V. Thus, the preamplifier has to be disconnected while heating. The XXF-1 electronics contains all circuitry needed and a convenient heater automatic controlling the heating duration between 1 ms and 4 s [18].

A total of 23 different double-transformer SQUIDs with  $L_{in}$  values between  $\approx 24 \text{ nH}$  and  $2 \mu\text{H}$  were realized on our latest mask set C4. The input inductance was varied by changing the number of turns in the input transformer while keeping the total inductance of the intermediate loop roughly constant. In addition to the integrated two-stage devices, single-stage SQUIDs with APF and BCF were implemented for applications with relaxed demands on the SQUID noise.

#### IV. SENSORS WITH LOW INPUT INDUCTANCE

We have designed a series of low-inductance sensors for the readout of cryogenic detectors or for use as second stage in discrete two-stage setups. Fig. 6 shows our latest array chip C4X16F which contains two independent 16-SQUID series arrays. Each array has a feedback coil and an input coil with  $L_{in} \leq 3 \text{ nH}$ . For convenience, rf filters as well as bias resistors for detector operation were integrated into the chip. We have

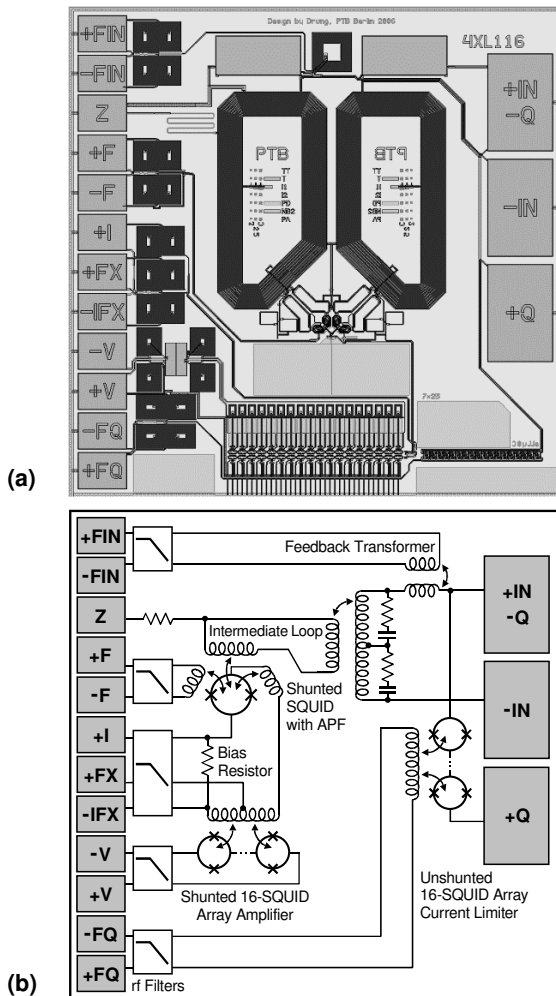


Fig. 5. (a) Layout and (b) basic circuit diagram of the integrated two-stage sensor C4XL116. Chip size is  $3 \text{ mm} \times 3 \text{ mm}$ . Circuit details (shunt resistors etc.) are omitted for clarity. Z is a test point for detecting shorts between the intermediate loop and the front-end SQUID or the input coil.

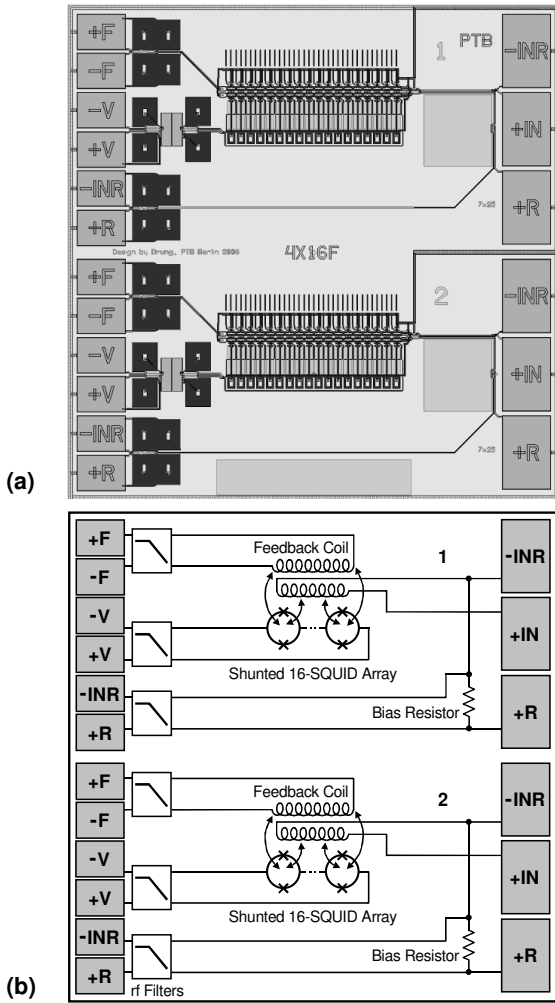


Fig. 6. (a) Layout and (b) basic circuit diagram of the 3 mm × 3 mm sensor chip C4X16F. The chip contains two independent 16-SQUID arrays. Circuit details (shunt resistors etc.) are omitted for clarity.

realized bias resistors with  $R_b = R/10 \leq 1 \Omega$  for two-stage setups, and bias resistors with nominal values of 50  $\Omega$ , 90 m $\Omega$ , 4 m $\Omega$  and 0.3 m $\Omega$  for detector readout. The flux noise level at 4.2 K is typically 0.4  $\mu\Phi_0/\sqrt{\text{Hz}}$  with a 1/f corner around 10 Hz, corresponding to a current noise level of 9 pA/ $\sqrt{\text{Hz}}$ . It decreases to 5 pA/ $\sqrt{\text{Hz}}$  when lowering the temperature to 300 mK, limited by the preamplifier noise contribution of the XXF-1 electronics [16]. For applications requiring a better energy resolution at low temperatures (at the expense of a reduced slew rate) we have realized two-stage sensors without input transformer. These devices have a lower input inductance of about 2 nH, and an improved current noise level of 6 pA/ $\sqrt{\text{Hz}}$  or 2 pA/ $\sqrt{\text{Hz}}$  at 4.2 K or 300 mK, respectively.

Our SQUID arrays are very robust and insensitive to magnetic fields. They can be cooled down in the Earth field and may be mounted directly on a Cu block at the cold stage of a mK cryostat without degradation in noise. Their power consumption of  $\approx 1$  nW per channel is acceptable in most applications. They are particularly interesting for applications where maximum dynamic performance is needed. However,

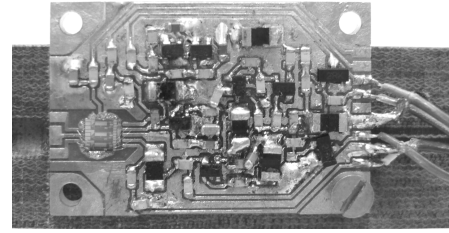


Fig. 7. Photograph of the 30 mm × 20 mm FLL board mounted on a dip stick with a fabric-base laminate holder.

when using a room temperature readout electronics, the achievable system bandwidth is limited to about 20 MHz by the propagation delay on the transmission lines [16].

The loop delay can be reduced strongly when using a flux-locked loop (FLL) electronics operated at 4.2 K in close proximity to the SQUID. However, until now the dynamic performance of such cold readout electronics was not competitive with that of fast room temperature electronics because of the limited performance of the semiconductor components at 4.2 K [19]. Recently, it was demonstrated that the Silicon-Germanium bipolar rf transistor BFP650 from Infineon works well at 4.2 K [20]. Stimulated by this, we have developed a prototype of an ultrafast cold readout electronics and connected it to a C3X16A array chip without on-chip rf filters (Fig. 7) [21]. In this way, the total loop delay was reduced to about 0.65 ns, and the system bandwidth was correspondingly increased to 350 MHz. As shown in Fig. 8, a

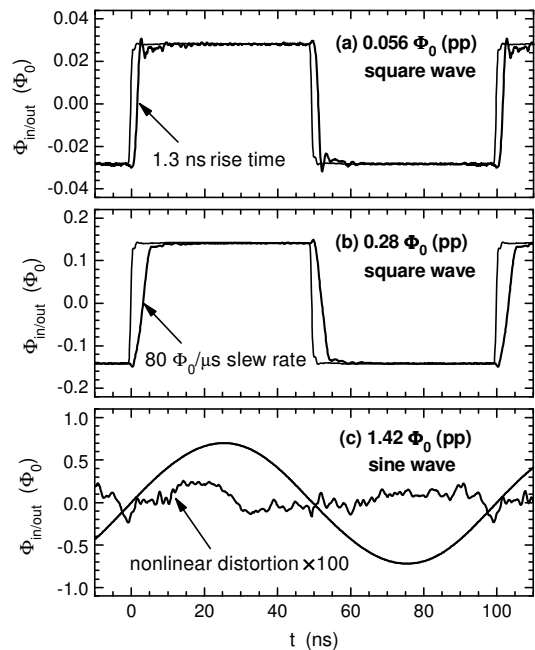


Fig. 8. Dynamic performance of the cold FLL: (a) Small-signal step response, (b) large-signal step response, and (c) nonlinear distortion at 10 MHz. The output traces in (a) and (b) were shifted by 8 ns to compensate for the delay in the transmission lines. To minimize noise effects, all output traces were averaged  $2^{16}$  times. Traces (c) were additionally filtered by a 80 MHz first-order low-pass. To display the distortion signal, the fundamental was removed by subtracting the input from the output with fine-tuned phase and amplitude.

small-signal rise time as low as 1.3 ns and a slew rate as high as  $80 \Phi_0/\mu\text{s}$  were achieved, which outperforms the dynamics of the fastest room temperature FLL by more than an order of magnitude [16]. The unity-gain bandwidth was 120 MHz, i.e., the loop gain was  $\approx 12$  at 10 MHz. Thus, a 10 MHz sine wave with a peak-to-peak amplitude of  $1.42 \Phi_0$  can be tracked with a low nonlinear distortion of 0.35% – see Fig. 8(c).

The cold FLL consists of two transistor stages acting as a high-gain amplifier and a buffer. The preamplifier voltage noise is  $\approx 0.2 \text{ nV}/\sqrt{\text{Hz}}$  with a  $1/f$  corner at about 100 kHz. The overall current noise of the array was  $8 \text{ pA}/\sqrt{\text{Hz}}$  close to the value obtained with the XXF-1 electronics. The total power consumption at 4.2 K was 10 mW which will be lowered to 6 mW in the next electronics version. The static dynamic range was set to  $\pm 13 \Phi_0$ .

## V. MAGNETIC FIELD SENSORS

We have also realized a few magnetic field sensors on our C4 mask set for applications where the large chip size ( $7.2 \text{ mm} \times 7.2 \text{ mm}$ ) of our “biomagnetic” multiloop magnetometers W9L [4] is undesirable or a higher dynamic range is needed (see Fig. 9). In order to allow direct readout, APF and BCF were integrated on-chip similarly to Ref. [12]. Stripline “spokes” have been used rather than coplanar “spokes” in order to maximize the field sensitivity [22]. A flux noise level of  $1.2 \mu\Phi_0/\sqrt{\text{Hz}}$  is achieved at 4.2 K, corresponding to  $3.6 \text{ fT}/\sqrt{\text{Hz}}$  or  $8.4 \text{ fT}/\sqrt{\text{Hz}}$  for the devices with 2.8 mm or 1.7 mm outer pickup coil dimension, respectively. Unfortunately, the low-frequency noise level of the first samples was relatively high for unknown reasons (about 10 Hz  $1/f$  corner). Nonetheless, considering the small loop size, the devices are very sensitive and useful for many applications.

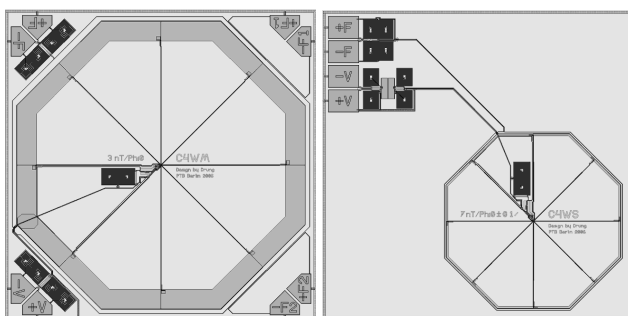


Fig. 9. Layout of the  $3 \text{ mm} \times 3 \text{ mm}$  magnetometer chips C4WM (left) and C4WS (right). The outer pickup coil dimensions are 2.8 mm and 1.7 mm for C4WM and C4WS, respectively.

## VI. CONCLUSION

We have developed a novel family of SQUID sensors which are highly adapted for today’s demanding SQUID applications. These sensors combine ease of use, low noise and high dynamic performance. A total of 47 different sensor chips are realized on our latest mask set C4 covering an input inductance range between about 1 nH and  $2 \mu\text{H}$ . All devices are optimized for direct readout using the XXF-1 electronics [16].

## ACKNOWLEDGMENT

The authors thank C. Günzel for SQUID preparation, K. Räther for fabrication of electronics boards, and C. Hinrichs and H.-J. Barthelmeß for fruitful discussions.

## REFERENCES

- [1] C. D. Tesche and J. Clarke, “dc SQUID: noise and optimization,” *J. Low Temp. Phys.*, vol. 29, pp. 301-331, November 1977.
- [2] R. Cantor and D. Koelle, “Practical dc SQUIDS: configuration and performance,” in *SQUID Handbook Volume 1*, J. Clarke and A. I. Braginski, Eds. Weinheim: WILEY-VCH, May 2004, pp. 171-217.
- [3] D. Drung, “High-performance DC SQUID read-out electronics,” *Physica C*, vol. 368, pp. 134-140, March 2002.
- [4] D. Drung, “High- $T_c$  and low- $T_c$  dc SQUID electronics,” *Supercond. Sci. Technol.*, vol. 16, pp. 1320-1336, December 2003.
- [5] R. P. Welty and J. M. Martinis, “A series array of dc SQUIDS,” *IEEE Trans. Magn.*, vol. 27, pp. 2924-2926, March 1991.
- [6] K. G. Stawiasz and M. B. Ketchen, “Noise measurements of series SQUID arrays,” *IEEE Trans. Appl. Supercond.*, vol. 3, pp. 1808-1811, March 1993.
- [7] G. Stan, S. B. Field, and J. M. Martinis, “Critical field for complete vortex expulsion from narrow superconducting strips,” *Phys. Rev. Lett.*, vol. 92, 097003, March 2004.
- [8] B. Muhlfelder, W. Johnson, and M. W. Cromar, “Double transformer coupling to a very low noise SQUID,” *IEEE Trans. Magn.*, vol. 19, pp. 303-307, May 1983.
- [9] V. Polushkin, E. Gu, D. Glowacka, D. Goldie, J. Lumley, “A tightly coupled dc SQUID with an intermediary transformer,” *Physica C*, vol. 367, pp.280-284, February 2002.
- [10] D. Drung, C. Afmann, J. Beyer, M. Peters, F. Ruede, and Th. Schurig, “dc SQUID readout electronics with up to 100 MHz closed-loop bandwidth,” *IEEE Trans. Appl. Supercond.*, vol. 15, pp. 777-780, June 2005.
- [11] K. D. Irwin and G. C. Hilton, “Transition-Edge Sensors,” in *Cryogenic Particle Detection*, C. Enss, Ed. Berlin: Springer, July 2005, pp. 63-149.
- [12] D. Drung and H. Koch, “An electronic second-order gradiometer for biomagnetic applications in clinical shielded rooms,” *IEEE Trans. Appl. Supercond.*, vol. 3, pp. 2594-2597, March 1993
- [13] F. C. Wellstood, C. Urbina, and J. Clarke, “Low-frequency noise in dc superconducting quantum interference devices below 1 K,” *Appl. Phys. Lett.*, vol. 50, pp. 772-774, March 1987.
- [14] R. P. Welty and J. M. Martinis, “Two-stage integrated SQUID amplifier with series array output,” *IEEE Trans. Appl. Supercond.*, vol. 3, pp. 2605-2608, March 1993.
- [15] R. Cantor, A. Hall, and V. Zotev, “High-Speed two-Stage SQUID amplifiers for cryogenic detector readouts,” presented at 2nd International Workshop on Transition Edge Sensor Device Physics, Coral Gables, Florida, USA, March 18-19, 2004. Available: <http://origins.colorado.edu/~deiker/tes/2004/talks/Cantor.pdf>.
- [16] D. Drung, C. Hinrichs, and H.-J. Barthelmeß, “Low-noise ultra-high-speed dc SQUID readout electronics,” *Supercond. Sci. Technol.*, vol. 19, pp. S235-S241, May 2006.
- [17] G. Uehara, N. Matsuda, K. Kazami, Y. Takada, and H. Kado, “Asymmetric bias injection technique for Drung-type superconducting quantum interference devices,” *Jpn. J. Appl. Phys.*, vol. 32, pp. L1735-L1738, December 1993.
- [18] Manual of XXF-1 electronics, Magnicon GbR, Lemsahler Landstraße 171, D-22397 Hamburg, Germany; <http://www.magnicon.com>
- [19] M. Mück, M. Korn, C. G. A. Muford, and J. B. Kycia, “Cryogenic direct current superconducting quantum interference device readout circuit,” *Rev. Sci. Instrum.*, vol. 76, pp. 074701-074705, July 2005.
- [20] M. Kiviranta, A. Virtanen, H. Seppä, J. Penttilä, J. Hassel, and P. Helistö, “A post-SQUID ac amplifier aimed for multiplexed detector readouts,” *Supercond. Sci. Technol.*, vol. 19, pp. S371-S375, May 2006.
- [21] D. Drung, C. Hinrichs, and H.-J. Barthelmeß, “An ultrafast SQUID electronics operated at 4.2 K,” paper 3EJ02 at ASC 2006, Seattle, Washington, USA, August 27 – September 1, 2006 (unpublished).
- [22] D. Drung, S. Knappe, and H. Koch, “Theory for the multiloop dc superconducting quantum interference device magnetometer and experimental verification,” *J. Appl. Phys.*, vol. 77, pp. 4088-4098, April 1995.